

Design for a Time Variance - Gravitational Wave Detector

Peter CM Hahn
email: petehahn@telus.net
June 3, 2016

Abstract

This article describes a unique design for a device that will detect gravitational waves directly. The technique used in this design is based on the *inflow* that is predicted by Foamy Ether Theory (FET). Unlike current interferometer-based detectors that claim to measure distortions of space caused by gravitational waves, the proposed Time Variance - Gravitational Wave Detector (TV-GWD) measures changes in the rate-of-flow-of-time.

The TV-GWD has the capability of detecting much higher frequencies than interferometer-based detectors because it measures fluctuations in time instead of distortions in space. The TV-GWD can be mounted on a tabletop instead of kilometer-length antennas that are required by interferometers.

Details of the design and tests performed are presented. Photos of an actual working prototype are also provided.

Keywords: gravitational waves, gravitational wave detector, general relativity, Foamy Ether Theory

Table of Contents

Introduction.....	2
TV-GWD Design Description.....	3
Laser	3
Optic Components	4
Linear Array Photo Sensors.....	4
Wavelength Calculation	4
Digital Acquisition (DAQ)	6
<i>Anti-alias Filter</i>	7
<i>Master Clock</i>	7
<i>Analog to Digital Conversion</i>	8
<i>Signal Preprocessing</i>	8
Data Collection and Storage	9
System Monitoring	10
Signal Processing and Analysis (DSP).....	10
Test Signal Injection System Description	13
Test Signal Injection Results	14
Chirp Signal.....	14
Pulsar Signal.....	15
Techniques to Enhance Detector Performance	16
Increase Sensitivity	16
Increase Bandwidth.....	17

Add Directionality.....	17
Alternate Configuration	17
Conclusion	18
Current TV-GWD Prototype Photos.....	19
References.....	20

Introduction

According to Einstein’s general theory of relativity, compact massive astronomical objects in motion will generate gravitational waves. These gravitational waves cause distortions in the fabric of space-time that ripple outwards at the speed of light. A number of gravitational wave detectors (such as LIGO¹, VIRGO² and GEO600³) are currently in operation. These detectors are based on a laser interferometer configuration that are designed to detect minute distortions in space. Although these detectors have been in operation for a number of years and many enhancements have been made, no valid gravitational waves have been detected to date that have been confirmed by follow-up observations^{4 5}.

[Foamy Ether Theory](#) (FET)⁶, however, claims that interferometer-based gravitational wave detectors are fundamentally flawed, and predicts that they will continue to produce null results, regardless of any sensitivity improvements. [FET](#) explains the reasoning behind this prediction by showing that the speed of light increases^{7 8} and the wavelength increases⁹ in proportion to the stretching of space. This results in the returned laser light *a/ways* being in phase, thereby generating no light at the interferometer’s photo-detector.

This article proposes the unique and innovative design of a device that will be able to directly detect gravitational waves. The technique used in this design is based on the *inflow*¹⁰ that is predicted by FET.

This new Time Variance - Gravitational Wave Detector (TV-GWD) design is based on the premise that incoming gravitational waves will cause a variation in the rate-of-flow-of-time. This [variation](#) is explained in detail on the FET site, which states that incoming gravitational waves will cause a variance in the downward flow of ether at the earth’s surface. This will result in a fluctuation in the rate-of-flow-of-time.

The TV-GWD is also based on the principle that the diffraction pattern generated by a monochromatic light source (laser), traveling through a multiple slit device, can be used to accurately measure the laser’s wavelength (see Figure 1). Any change in the rate-of-flow-of-time will also correspondingly cause a change in the laser’s frequency (and wavelength). This will cause the peaks and troughs of the interference pattern to stretch or compress in the horizontal direction. Linear array sensors placed at the left and right peaks of this pattern are able to detect

changes in the interference pattern, thereby sensing a change in the laser's wavelength (see Figure 2). The signals from these two linear array sensors are sent to a Digital Acquisition System (DAQ) for real-time data capture and storage. Captured data can then be analyzed later by Digital Signal Processing software.

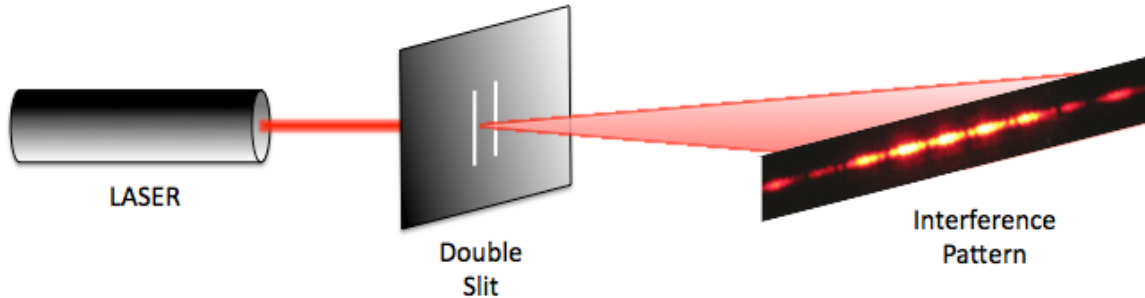


Figure 1

TV-GWD Design Description

Time Variance – Gravitational Wave Detector

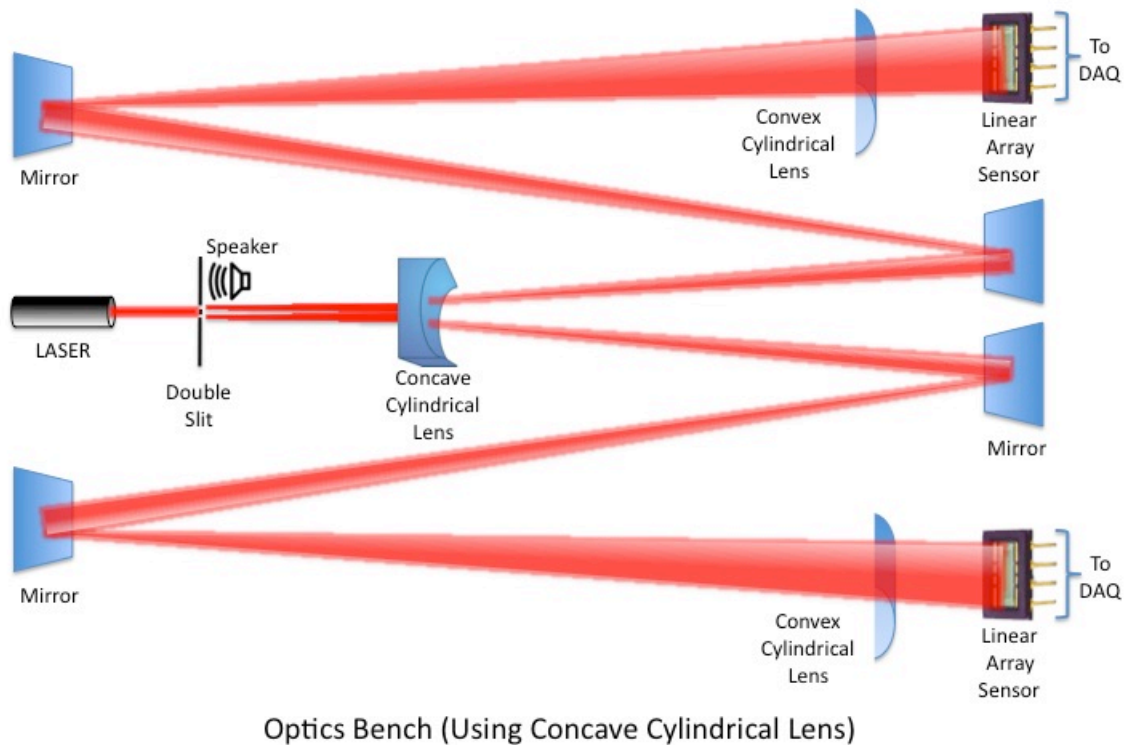


Figure 2

Laser

A 2 mW Helium Neon Laser¹¹ was chosen to generate a coherent, monochromatic light beam at a wavelength of 632.8 nm.

Optic Components

The HeNe laser is aimed at a multi-slit diffraction grating that generates an interference pattern (as shown in Figure 3).

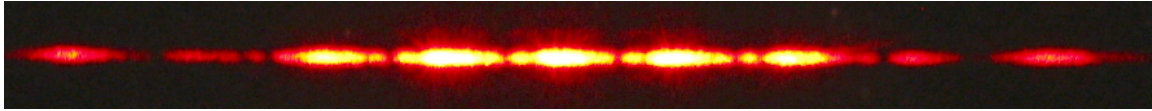


Figure 3

The current prototype uses a PASCO High Precision Diffraction Slit¹², currently set at five slits. The slit width is 0.04mm and slit spacing is 0.125mm. The laser light travels through a concave cylindrical lens, which spreads out the diffraction pattern in the horizontal direction. Flat mirrors are used to extend the path length of the laser light. (The combined use of a concave cylindrical lens and flat mirrors result in a path length equivalent to 10 meters in the current prototype.) The diffraction pattern then passes through a convex cylindrical lens that vertically focuses the bright nodes onto a linear array sensor.

Linear Array Photo Sensors

A 512x1 pixel linear array sensor¹³ is used to capture the diffraction pattern and convert it into an analog signal. The sensor in use has a pixel pitch of 12.5 μm and a pixel height of 250 μm . The clock speed is set at 512 pixels multiplied by 4096 lines per second, or 2.097MHz. (The line rate was set to 4096 lines per second for future compatibility with LIGO Open Science Center¹⁴ data processing algorithms).

Wavelength Calculation

Referring to Figure 4, we can derive the Fraunhofer diffraction equation for maximum brightness locations of the nodes.

$$y = \frac{m\lambda D}{d} \quad \text{Equation 1}$$

Where:

y is the distance from the center to a bright node

λ is the wavelength of the laser light

m are integer numbers (0,1,2,3...)

D is the distance between the slits and the screen

d is the distance between slits

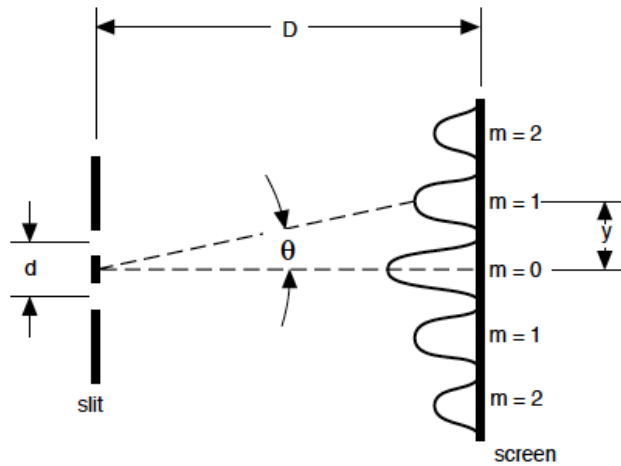


Figure 4
Source: PASCO doc. 012-05880D

The linear array sensors are positioned at the two locations where $m=2$ (of Figure 4). This enables the sensors to track any changes in the wavelength of the laser light. According to FET, a gravitational wave passing through the TV-GWD will cause a fluctuation in the rate-of-flow-of-time, which will correspondingly cause a fluctuation in the laser's wavelength. This change in wavelength will cause the distance y to fluctuate as well. The actual distance y is of secondary importance; the detector is designed to focus primarily on the *changes* in y . Figure 5 shows the diffraction patterns generated from multiple slit devices. (One can see that more slits results in narrower bright spots.)

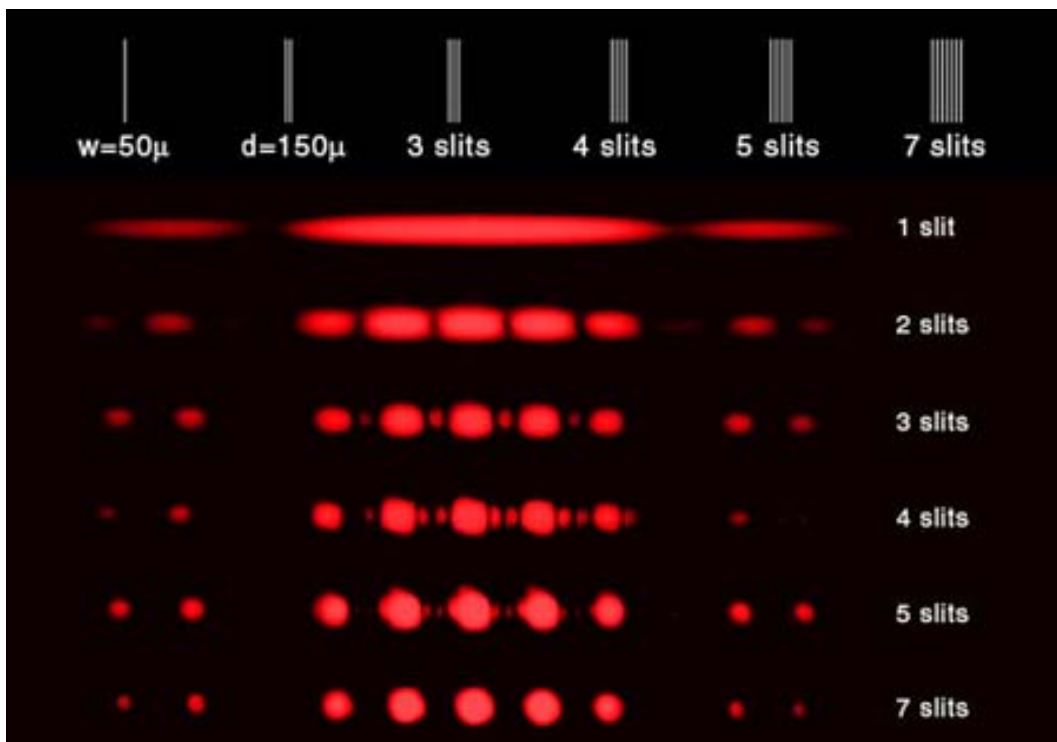


Figure 5
Source: University of Tennessee¹⁵

This configuration has the added benefit of being insensitive to laser power fluctuations because the *horizontal position* of the node is important, not its brightness.

More information on calculating wavelengths is available at [HyperPhysics](#)¹⁶.

Digital Acquisition (DAQ)

The two linear array sensors capture the diffraction pattern and produce analog signals as shown below. Figure 6 is a sample of the left sensor and Figure 7 is a sample of the right sensor. The diffraction pattern is sampled 4096 times per second. The time duration between peaks is $1/4096\text{Hz}$ or $244.14\mu\text{s}$.

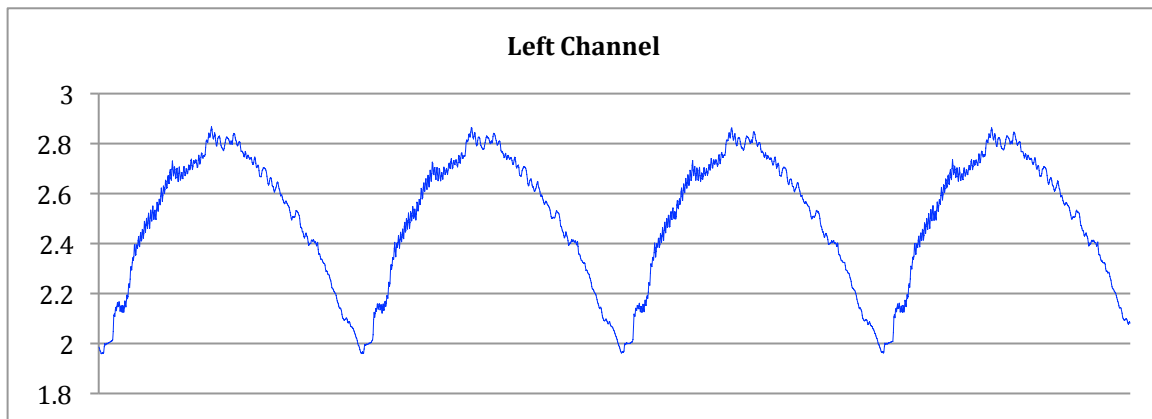


Figure 6

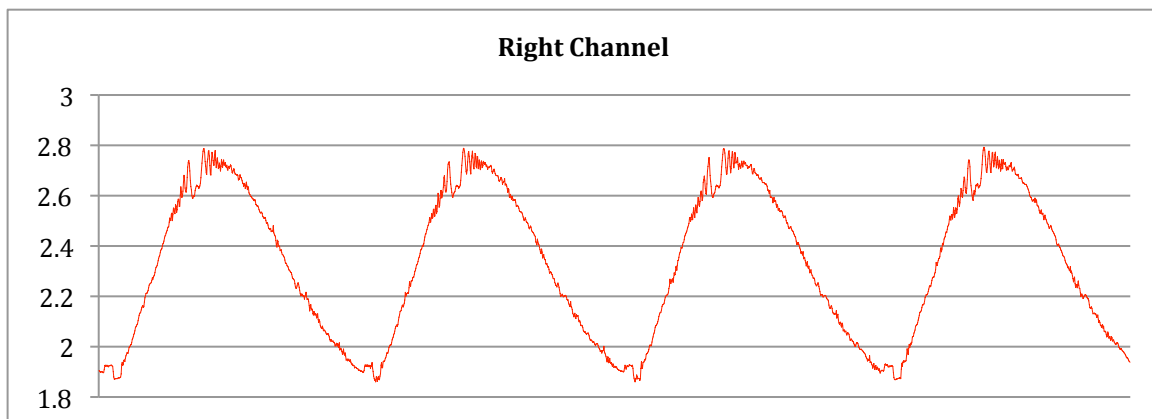


Figure 7

Figure 8 below shows a block diagram displaying components of the Data Acquisition System (DAQ). Analog signals from the left and right linear array sensors feed into an anti-alias filter, which are then converted to digital format at the Analog to Digital Converter (ADC). Preprocessing modules capture the digital signals and send them to a data collection and storage system for later analysis.

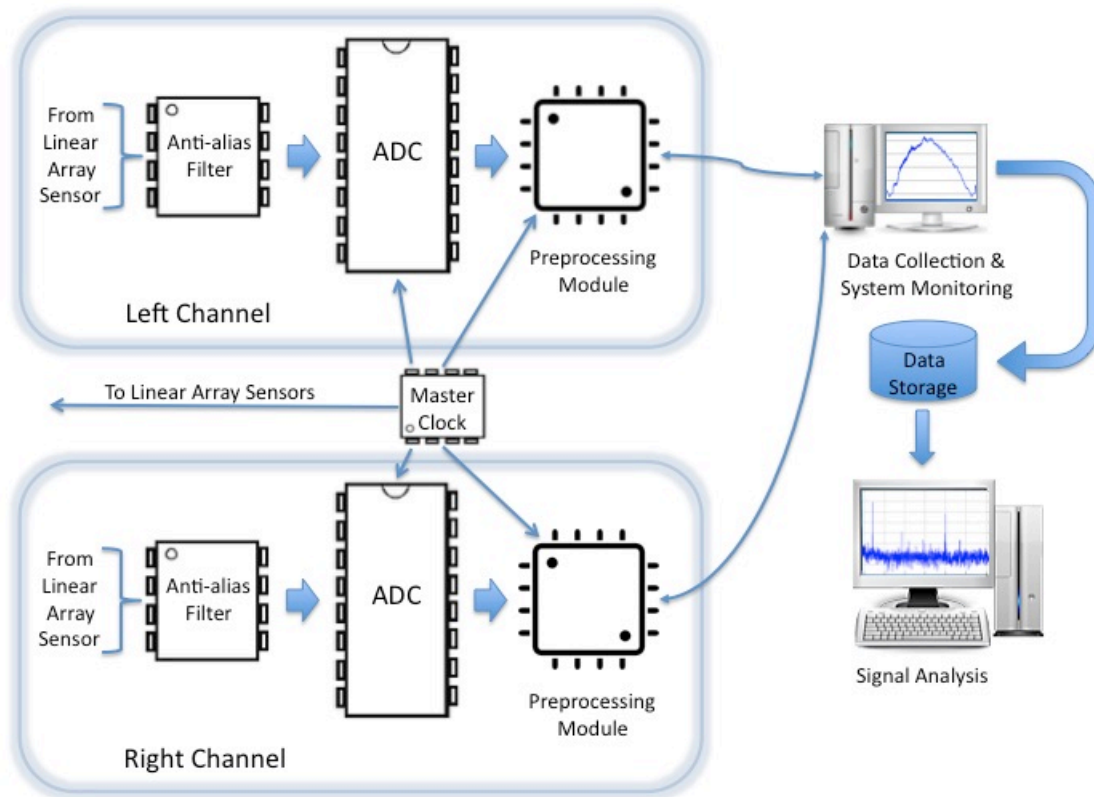


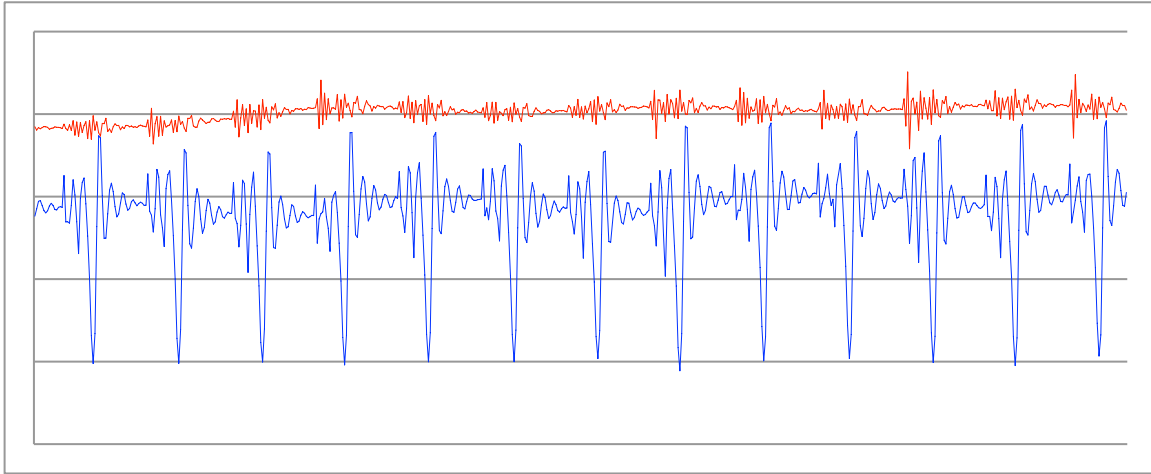
Figure 8
Data Acquisition (DAQ) and Analysis

Anti-alias Filter

An anti-aliasing filter is required to filter out any high frequency signals that are above the Nyquist frequency¹⁷. It is essentially a low-pass filter set to attenuate frequencies above the Nyquist frequency (half the sample rate). The blue line in Figure 9 shows a sample of a signal entering the anti-alias filter; the red line shows the signal leaving the anti-alias filter. The linear array sensors are being sampled at 2.097MSPS (Mega Samples Per Second), so the anti-alias filter was set to the Nyquist frequency of 1MHz. The filter used in the current prototype is an LTC1560-1 from Linear Technology¹⁸.

Master Clock

The startKIT¹⁹ development board from XMOS²⁰ was chosen as the platform for generating clocking signals. The CPU runs at 100MHz, which allows the clocking signals to be programmed in increments of 10ns. The master clock provides clocking and synchronization signals to the linear array sensors, ADC's and preprocessors.



Analogue to Digital Conversion

The signal passes from the anti-alias filter to an ADC. The ADC is connected to the master clock so that its analogue to digital conversion is synchronized with the linear array sensors (clocking at 2.097 MSPS). The digital signal is then sent to the preprocessor via a 10 bit parallel bus. The ADC used is the 10-Bit AD9051 from Analog Devices²¹.

Signal Preprocessing

The startKIT development board from XMOS was also chosen for the preprocessor platform. It has a 32 bit, 8 core CPU running at 100MHz. The multi core CPU allows multiple processes to run simultaneously, which is essential for the time critical nature of streaming data.

The preprocessor captures digital samples from the ADC at a rate of 2.097MSPS. The linear array sensors contain 512 pixels, so each frame (or line) contains 512 samples and takes 244.14 μ Sec to transmit. The bright node of a diffraction pattern produces an image that is very bright in the middle and dimmer around the edges. Figure 10 shows a plot of a typical node after being scanned.

The plot shown in Figure 10 looks identical to a histogram²², so the preprocessor is programmed to capture each frame and calculate the mean of the histogram of that frame. Calculating the mean of the histogram is key to the operation of the detector. The varying frequency of the laser light causes the diffraction pattern to shift left and right on the linear array sensor, which in turn, causes the mean of the histogram (for each frame) to vary as well. (If the optical components are aligned properly, the peak of a node of the diffraction pattern would be centered on pixel number 256 and the mean of the histogram would also be 512/2 or 256).

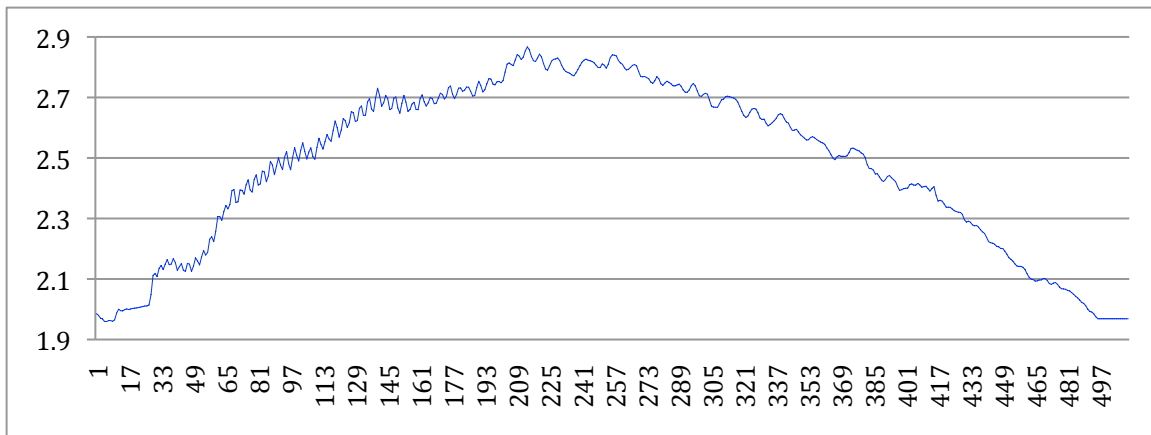


Figure 10
Frame Capture Sample

Equation for calculating the mean of a histogram:

$$\mu = \frac{1}{N} \sum_{i=0}^{M-1} iH_i$$

Equation 2

Where:

N is the number of points in the signal

M is the number of points in the histogram

H_i are the values of the sampled signal

C code for calculating the mean of a histogram (using xTIMEcomposer²³):

```

mean = 0, n = 0;
for(int i=0; i<512; i++){
    //read ADCportValue
    n = n + ADCportValue;
    mean = mean + i * ADCportValue;
}
mean = mean/n;

```

Figure 11

The preprocessor then sends the mean result of each frame to the data collection system through a GPIO Slice²⁴ card (via an RS232 interface).

Data Collection and Storage

The two RS232 cables are connected to USB converters, which are attached to USB inputs on a PC. RS232 Data Logger²⁵ is the software used to capture the incoming streaming data. Two instances of the program are run so that the left and right channels each get stored in their own individual files. The baudrate is set at 115200 with two 8-bit words representing a frame sample.

System Monitoring

The USB Oscilloscope²⁶ from Digilent is used to monitor the output of both linear array sensors and to align the optical components. Sensors from the oscilloscope are connected to the analog input of the ADCs. (The USB Oscilloscope was used to generate the plots in Figures 6, 7, 9 and 10).

Signal Processing and Analysis

Signal processing and analysis was primarily done using MATLAB²⁷ R2014a software. MATLAB's Signal Processing Toolbox²⁸ add-on was also used to provide additional signal processing capabilities. Figure 12 shows a typical sample of a time domain signal using MATLAB's Time Scope²⁹ system object. The plot shows that the signal has an approximate average peak-to-peak value of 50 (or 5 pixels). It also shows an additional low frequency drift that is caused by the instability of the laser. This low frequency component is not a problem since it occurs over several seconds, and downstream processing will remove it.

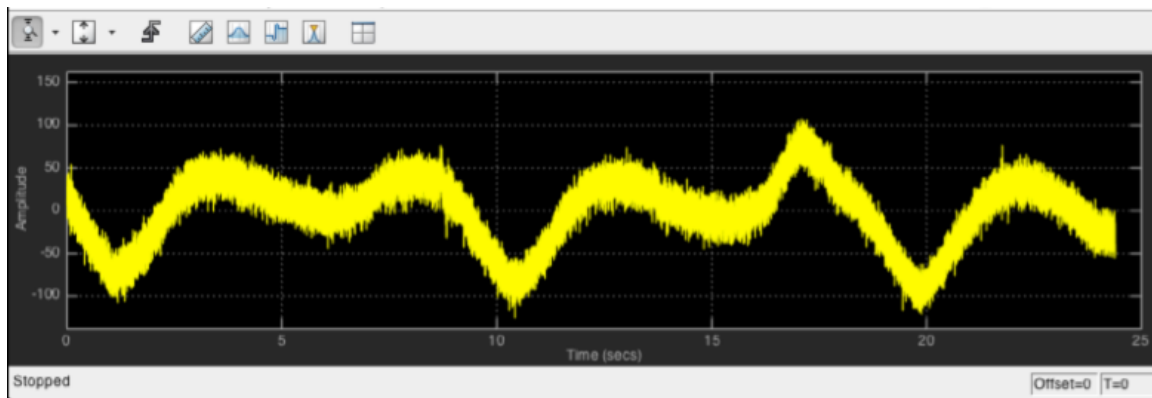


Figure 12

The following steps outline the downstream process:

1. Data files from the left and right channels are read simultaneously and the contents are converted from two 8-bit words to 16-bit integer values. As shown in Figure 13, each channel has its own unique noise signature.

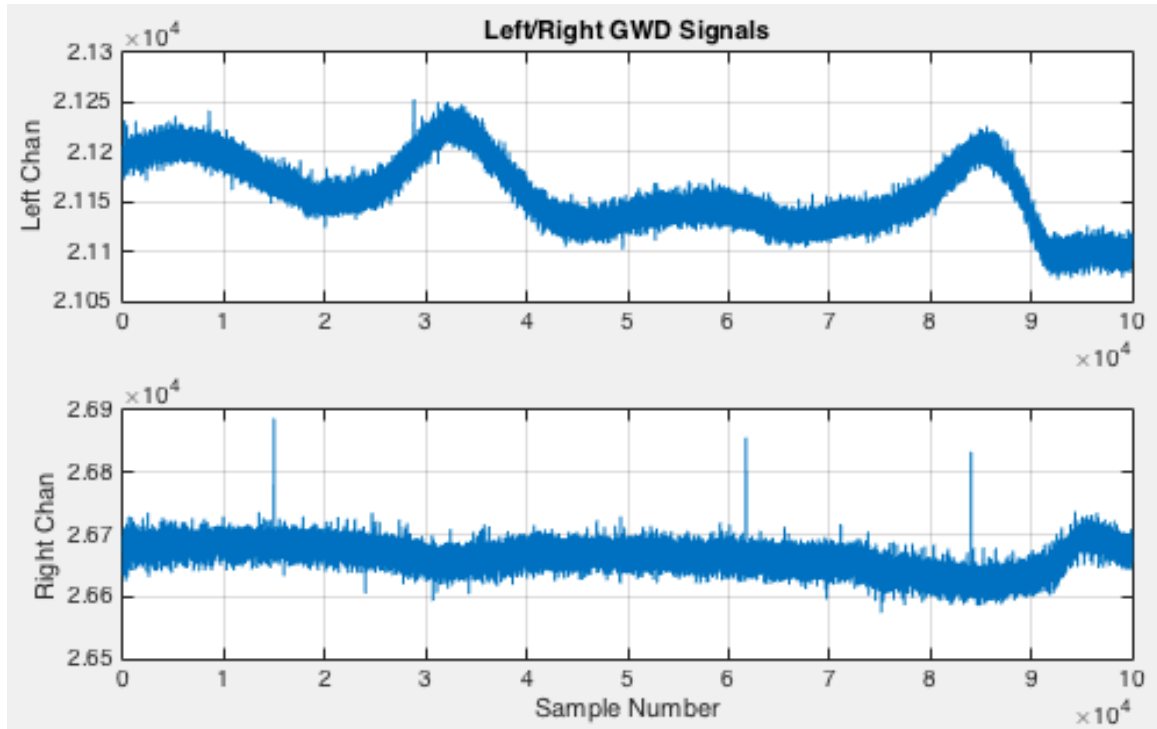


Figure 13

2. The `medfilt1`³⁰ function is used to remove unwanted, transient spikes, as shown below. Figure 14 shows what the right channel of Figure 13 looks like after the spikes are removed.

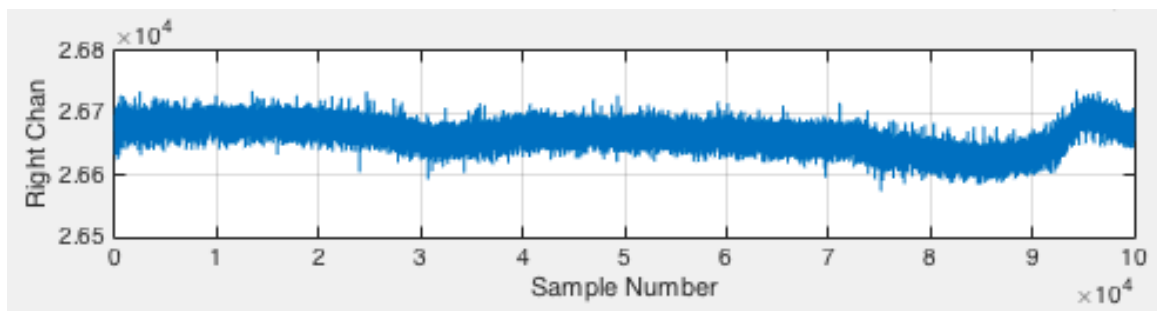


Figure 14

3. A `detrend`³¹ function is applied to remove the mean value or linear trend of the signal. This removes the DC component and centers the signal's pixel position to zero (Figure 15).

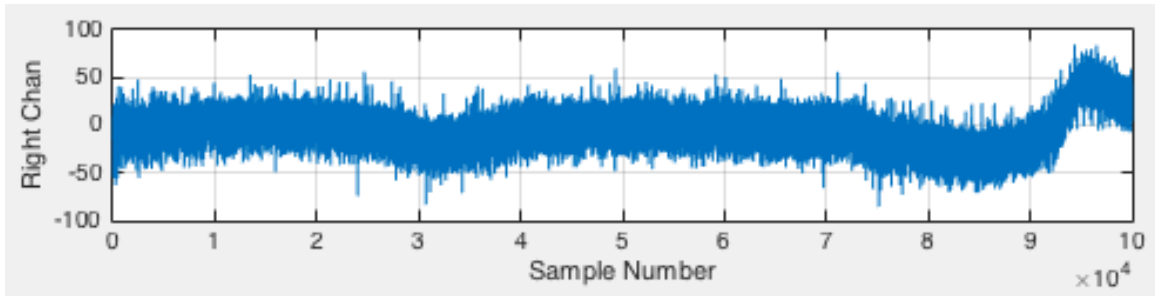


Figure 15

4. The left and right channels are then combined into one signal by a simple addition process. This has the benefit of reducing any random noise that may be present in an individual channel (Figure 16).

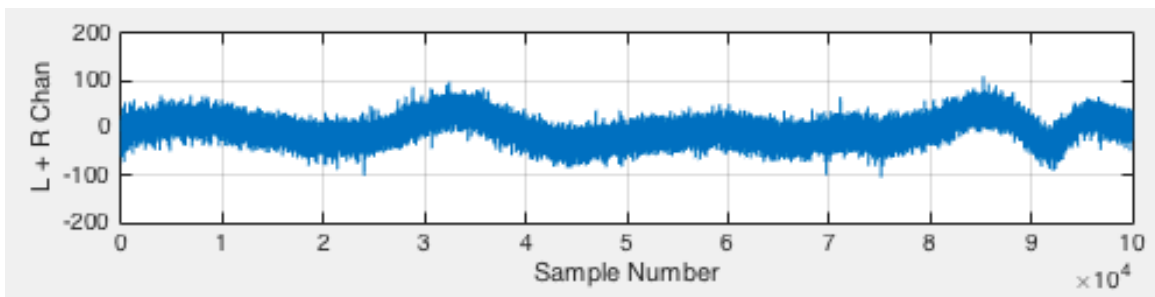


Figure 16

5. The `pwelch`³² function is used to return the power spectral density estimate of the combined signal. This is the function that is used to search for any periodic signals that may originate from compact objects such as pulsars or rotating black holes. Figure 17 shows a plot of the spectral density of the combined signal displayed in Figure 16.

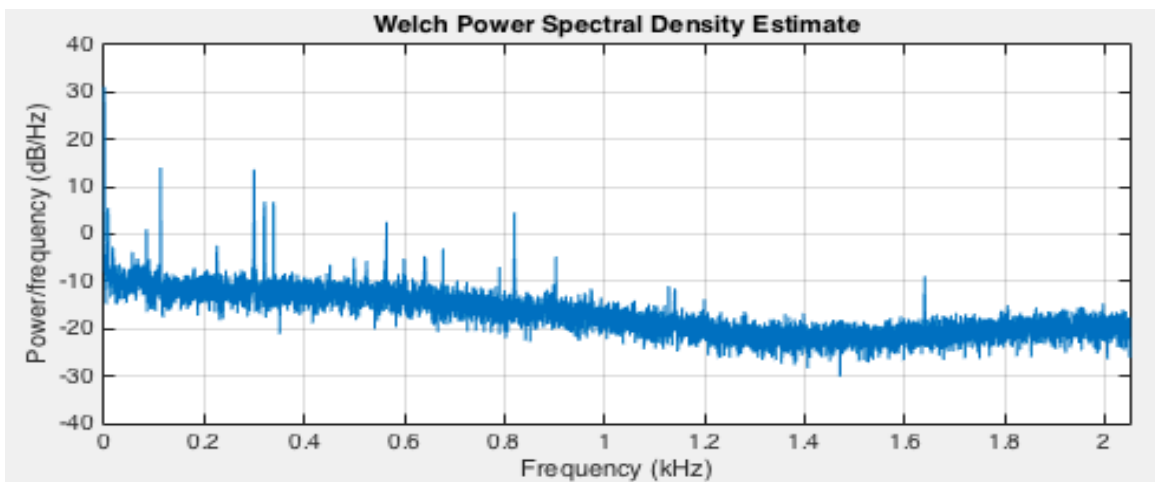


Figure 17

6. The `findpeaks`³³ function returns the numerical value of the local maxima (peaks) of the `pwelch` result. Table 1 below lists the frequencies and magnitudes of the peaks that are displayed in Figure 17.

Frequency	dB/Hz
0.250228868	1308.530032
8.007323772	3.59514839
8.632895941	1.111492025
84.70247177	1.266425128
112.9783338	25.55276858
299.6490693	23.41749771
319.9176076	2.569004906
320.2929509	3.704556926
320.9185230	4.894192194
338.6847727	4.808818956
564.3912115	1.807841486
820.2502289	2.863615053

Table 1

- The spectrogram³⁴ function returns the short-time Fourier transform of the input signal. This function shows a plot of the frequency power densities over a period of time. Figure 18 is a spectrogram of the signal displayed in Figure 16.

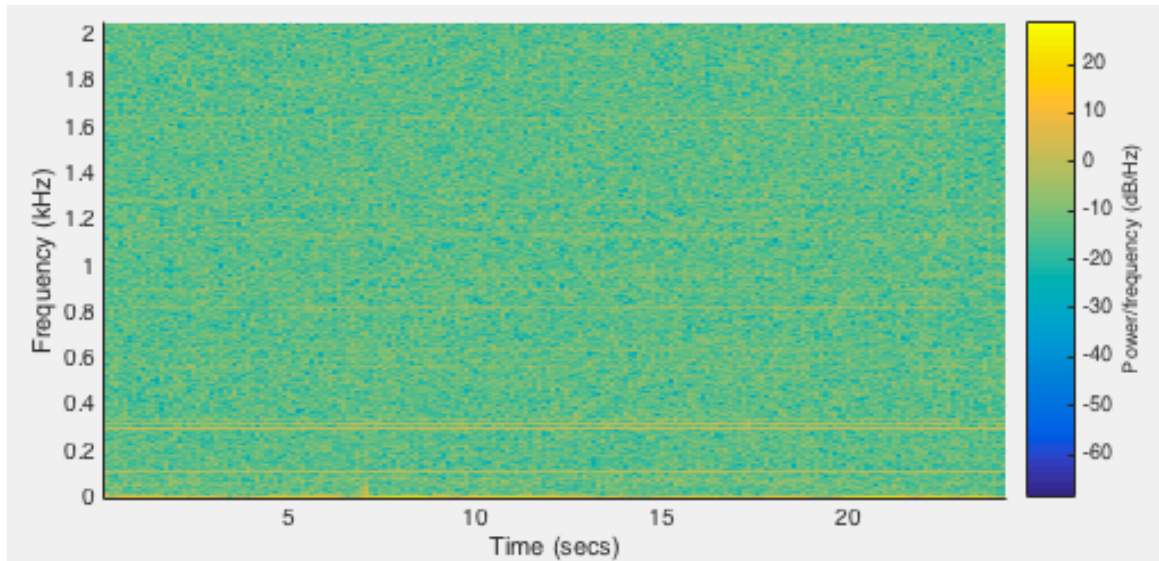


Figure 18

Test Signal Injection System Description

To simulate the detection of gravitational waves, test signals are injected into the detector by sending audio tones to a speaker system, which is mounted behind the double slit (see Figure 2). Audio tones from the speaker cause the double slit apparatus to vibrate slightly, resulting in minute changes in the distance between the double slit and the linear array sensor. This mimics variations in the frequency of the laser caused by gravitational waves. Referring to Equation 1

and Figure 4, one can see that a change in distances between nodes y is caused by a change in wavelength λ as well as a change in the distance D . This results in the test signal varying the interference pattern on the linear array sensor such that a change in y is directly proportional to a change in distance D .

Test Signal Injection Results

Chirp Signal

A chirp signal is generated when two compact objects, such as neutron stars or black holes merge. The chirp waveform is a unique signal type where both the amplitude and frequency increase with time until the two objects finally merge into one body. An example of this type of signal is shown in Figure 19 below.

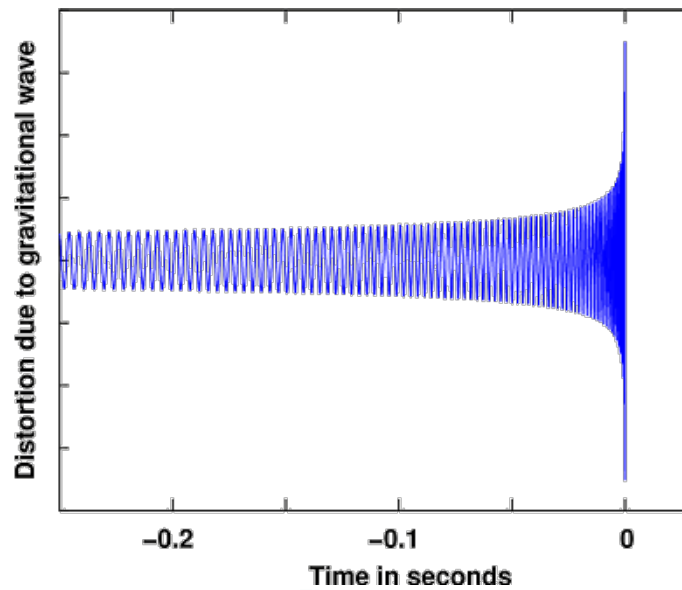


Figure 19
Chirping Neutron Stars³⁵

MATLAB's spectrogram function is ideal for analyzing and plotting chirp signals. Figure 20 below is a test run sample of a chirp signal that was injected into the detector. The audio test signal was acquired from the Einstein online website³⁶ and injected into the speaker system (see Figure 2). The result is displayed in Figure 20 below, which shows the frequency increasing with time until the merger is complete.

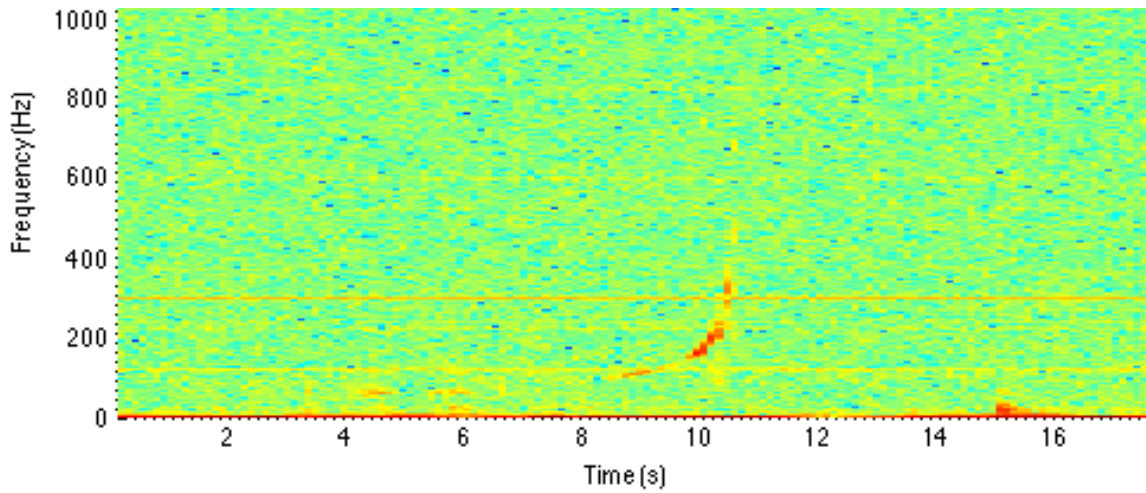


Figure 20
Spectrogram of Chirp Signal Injected Into TV-GWD

Pulsar Signal

Gravitational waves generated from pulsars are assumed to be extremely periodic, similar to their electromagnetic counterparts. To test the responsiveness of the TV-GWD, a steady tone of 1kHz is injected into the speaker system. The spectral density plot in Figure 21 shows the 1kHz tone, as well as its 2kHz harmonic. Figure 22 shows another plot of an injected signal using a 2kHz test tone.

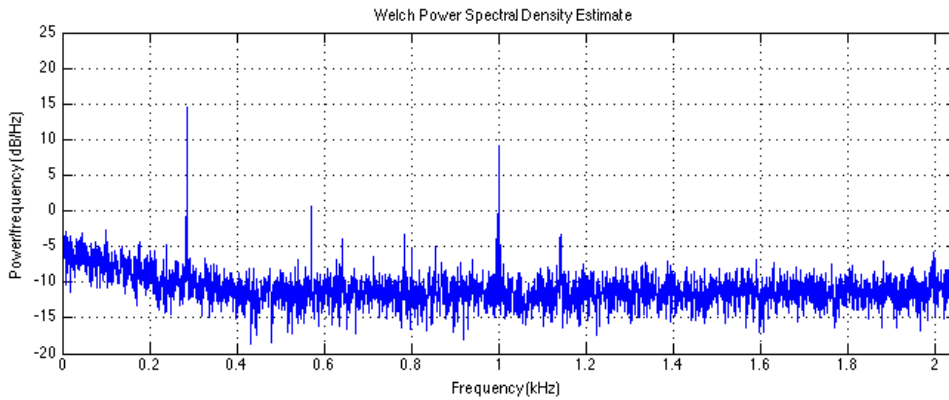


Figure 21
1kHz Test Tone (with faint 2kHz harmonic)

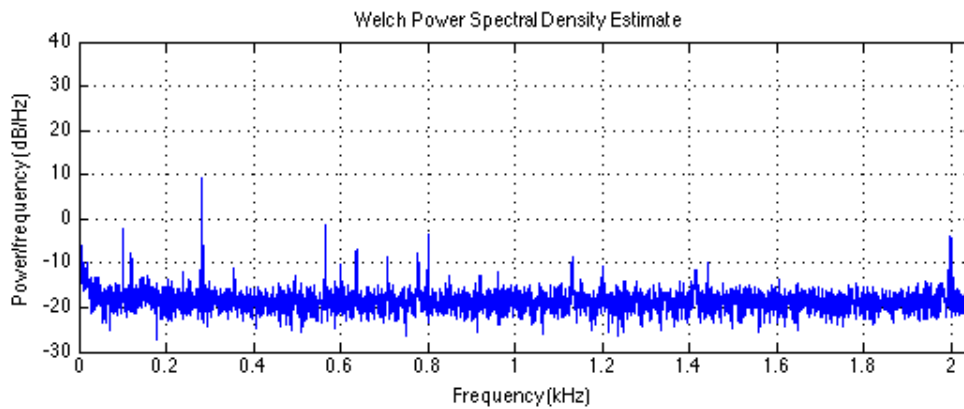


Figure 22
2kHz Test Tone

Techniques to Enhance Detector Performance

The prototype described in this article was built to test the validity of the design principles behind time variance measurement. Although test signal injections have shown that the TV-GWD is indeed capable of recording these fluctuations in time, a significant increase in sensitivity is required to detect gravitational waves from astrophysical sources.

The following is a list of detector enhancements that will improve performance, thereby increasing the TV-GWD's sensitivity and bandwidth.

Increase Sensitivity

The following enhancements could be made to increase the TV-GWD's sensitivity (thereby increasing its range):

1. Use a denser linear array sensor to detect smaller horizontal movements of the diffraction pattern
 - a. Use sensors that have a smaller pixel width.
 - b. Use sensors that have a larger number of pixels. This would allow the sensors to be positioned farther away from the slits.
2. Increase the distance between double slit and linear array sensors, thereby increasing the angular resolution.
3. Decrease the focal length of the concave cylindrical lens. This will cause the diffraction pattern to spread out more in the horizontal direction.
4. Use a higher bit count on the A/D converter to improve the resolution of the analog signal received from the linear array sensor.
5. Exchange the analog linear array sensor with one that has a digital output will reduce the component count, thereby reducing circuit noise.
6. Increase master clock stability. The current detector uses the crystal oscillator built into the XMOS startKIT. (Typically a crystal oscillator has a stability of only +/- 10 ppm).
7. Use a frequency-stabilized laser to reduce random fluctuations in laser wavelength.
8. Use a laser with a shorter wavelength to create a finer diffraction pattern.
9. Decrease the distances between slits to create a finer diffraction pattern.

10. Add more slits or a diffraction grating to reduce the width of the bright spots (see Figure 5).
11. Increase the seismic isolation of the optical bench to reduce vibrations caused by external sources.
12. Improve the AC isolation from DC power sources to reduce electronic circuit noise.
13. Arrange three collocated detectors in x, y, z configuration. This will allow for downstream processing to remove random variations in individual detectors.
14. Add microphones to monitor external sound interference. Downstream processing can then subtract external noise from detector signals.
15. Add seismic sensors (accelerometers). Downstream processing can then subtract external seismic noise from detector signals.
16. Monitor and control the temperature of the laser and detector.

Increase Bandwidth

The following enhancements could be made to increase the detector's bandwidth:

1. Install linear array sensors that have faster line rates (current sensors are limited to 9434 line scans per second).
2. Install faster A/D converters.
3. Replace the RS232 interface with higher speed links (i.e. USB, Ethernet).
4. Increase the laser power to allow for a shorter exposure (integration) time of the linear array sensors, which can then be scanned at a faster rate.

The upper frequency limit of the TV-GWD is basically determined by how fast the linear array sensors can be scanned. Faster scanning results in the TV-GWD being able to detect higher frequency gravitational waves.

The bandwidth of the current prototype is approximately 70Hz to 2048Hz. Sensitivity of the detector is unknown at this time.

Add Directionality

A single TV-GWD is unable to determine the direction of the source signal, since it only measures changes in the rate of flow of time. A three dimensional array of at least four detectors is required in order to determine the direction of the source gravitational wave. Detectors should be positioned at the vertices of a tetrahedron configuration.

Alternate Configuration

An alternate configuration is planned that results in a decrease in the number of optical components (see Figure 23). A convex cylindrical mirror will replace the concave cylindrical lens and two of the flat mirrors, located between the linear array sensors (see Figure 2). The convex cylindrical mirror spreads out the diffraction pattern in the same way that the concave cylindrical lens does, but with less loss and fewer stray reflections. (Concave cylindrical mirrors were not readily available at the time of prototype development).

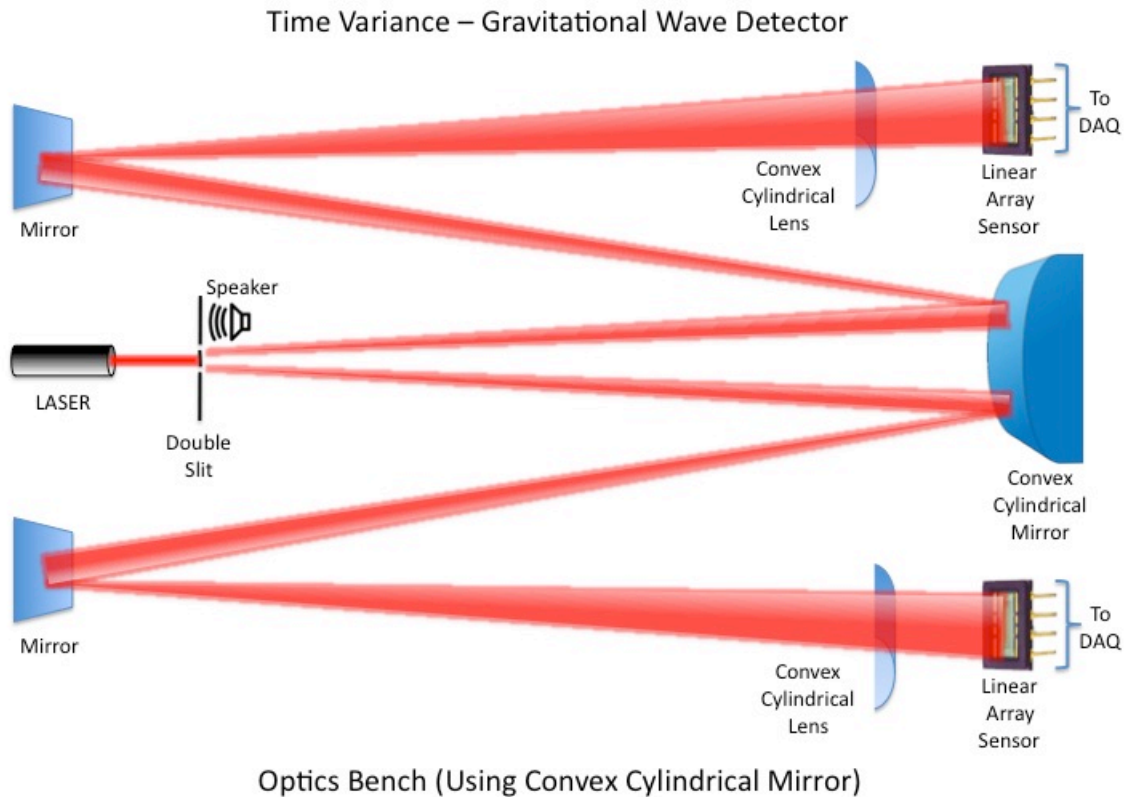


Figure 23

Conclusion

The TV-GWD offers an alternative design for a device that can be used to detect gravitational waves. Unlike current interferometer-based detectors that claim to measure distortions of space caused by gravitational waves, the TV-GWD measures changes in the rate-of-flow-of-time. And because of this, the TV-GWD design allows for greater sensitivity in the higher frequency ranges than can be achieved by interferometer-based detectors.

The TV-GWD also has the ability to validate ether inflow that is predicted by foamy ether theory. However, a minimum of two detectors on opposite sides of the Earth would be required to confirm this theory. As explained in FET, gravitational waves entering one side of the planet will experience a one hundred and eighty degree phase shift when leaving the opposite side.

In addition to analyzing gravitational waves originating from astrophysical sources, signals could also be analyzed for intelligent messages. Currently, projects such as *seti@home*³⁷ are looking for intelligent signals imbedded in electromagnetic (EM) waves. Advanced civilizations may have decided to use gravitational waves as their preferred method of interstellar communication. The high frequency capability of the TV-GWD would make it an ideal device for capturing these signals.

Current TV-GWD Prototype Photos

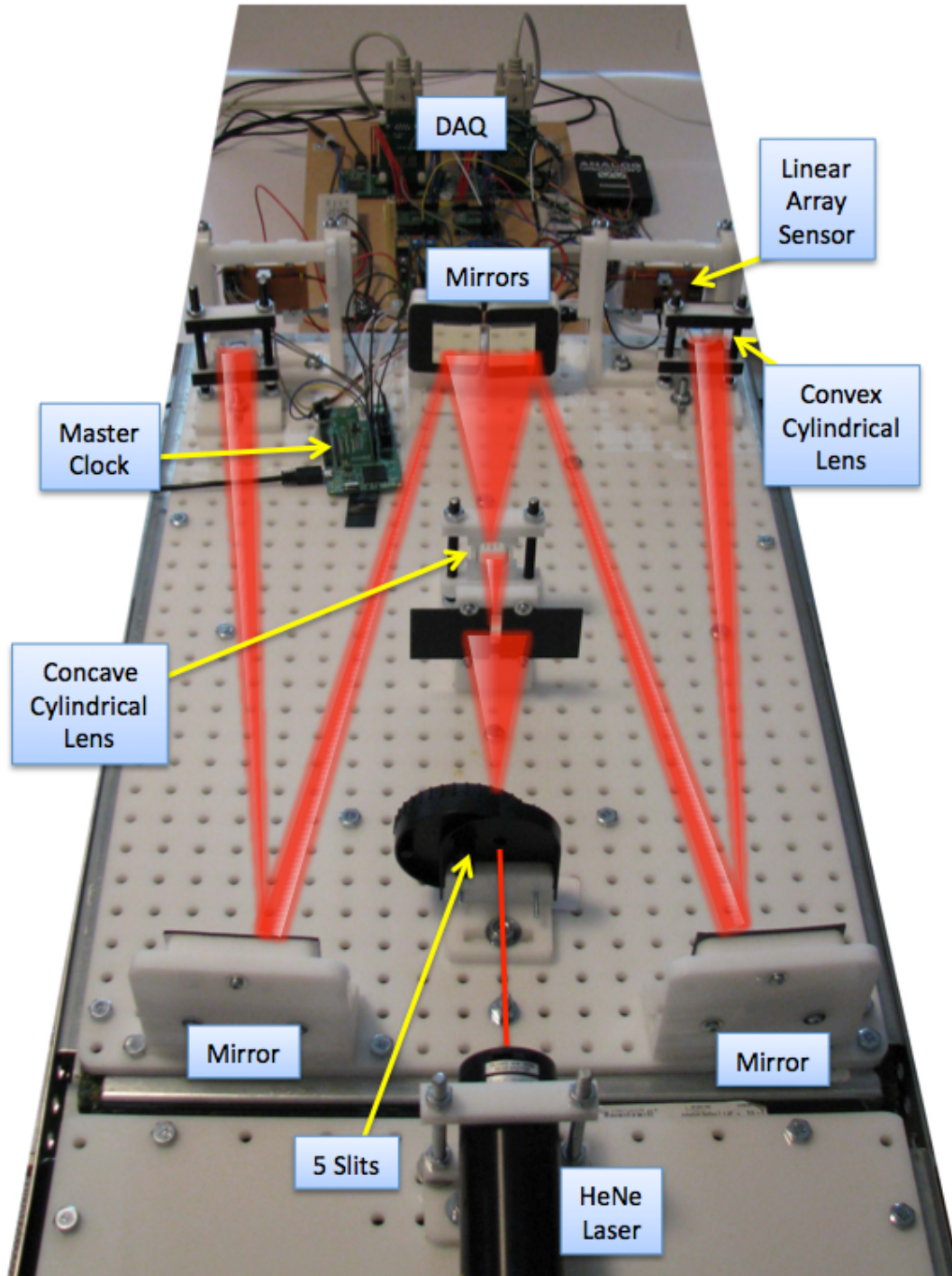


Figure 24
Photograph of the optical bench and DAQ

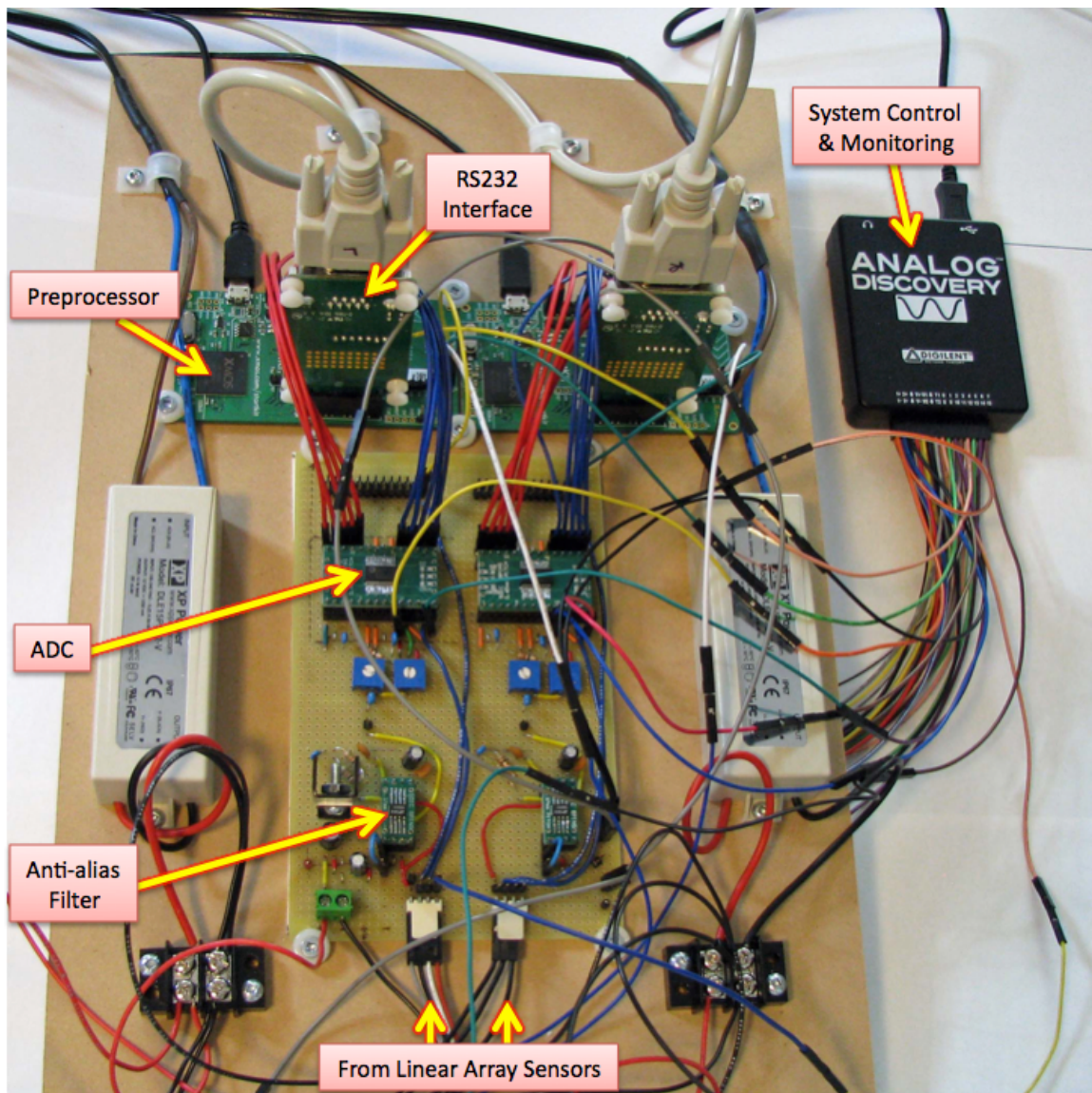


Figure 25
Photograph of the Data Acquisition Unit (DAQ)

References

¹ LIGO, Laser Interferometer Gravitational-Wave Observatory, May 2015, URL www.ligo.caltech.edu

² VIRGO, European Gravitational Observatory, May 2015, URL www.ego-gw.it/public/virgo/virgo.aspx

³ GEO600 Gravitational Wave Detector, May 2015, URL www.geo600.org

⁴ B. P. Abbott, R. Abbott, (1486 additional authors not shown), Localization and broadband follow-up of the gravitational-wave transient GW150914, arXiv:[1602.08492](https://arxiv.org/abs/1602.08492) [astro-ph]

-
- ⁵ B. P. Abbott, R. Abbott, (1520 additional authors not shown), Supplement: Localization and broadband follow-up of the gravitational-wave transient GW150914, arXiv:[1604.07864](https://arxiv.org/abs/1604.07864) [astro-ph]
- ⁶ Peter CM Hahn, Foamy (A)ether Theory – A Framework for a Theory of Everything, May 2015, URL www3.telus.net/foamyether
- ⁷ Alexander Unzicker, Jan Preuss, A Machian Version of Einstein's Variable Speed of Light Theory, arXiv:[1503.06763](https://arxiv.org/abs/1503.06763)
- ⁸ Alexander Unzicker, Einstein's Lost Key: How We Overlooked the Best Idea of the 20th Century, CreateSpace Independent Publishing Platform, 2015, ISBN 1519473435
- ⁹ Valerio Faraoni, A common misconception about LIGO detectors of gravitational waves, arXiv:[0702079](https://arxiv.org/abs/0702079) [gr-qc]
- ¹⁰ P.C. Hahn, Ether Inflow, (2016),
URL www3.telus.net/foamyether/etherinflow-grav.html
- ¹¹ THOR LABS, 2 mW Helium Neon Laser, April 2015, [HNL020L](https://www.thorlabs.com/newgrouppage9.cfm?id=1111)
- ¹² PASCO, High Precision Diffraction Slits, March 2015, ([OS-8453](https://www.pasco.com/products/physics/optics/diffraction-slits)).
- ¹³ Hamamatsu, linear array sensor, March 2015, [S9227-03](https://www.hamamatsu.com/usa/web/products/linear-array-sensors)
- ¹⁴ Michele Vallisneri, Jonah Kanner, Roy Williams, Alan Weinstein, Branson Stephens, The LIGO Open Science Center, arXiv:[1410.4839v2](https://arxiv.org/abs/1410.4839v2) [gr-qc]
- ¹⁵ University of Tennessee, Department of Physics and Astronomy, Diffraction and Interference, June 2015,
URL labman.phys.utk.edu/phys136/modules/m9/diff.htm
- ¹⁶ Georgia State University, Department of Physics and Astronomy, HyperPhysics, May 2015,
URL [hyperphysics.phy-astr.gsu.edu/hbase/phyopt/mulslidi.html - c2](http://hyperphysics.phy-astr.gsu.edu/hbase/phyopt/mulslidi.html)
- ¹⁷ Steven W. Smith, The Scientist and Engineer's Guide to Digital Signal Processing, ISBN 0-9660176-3-3, ch3, p41
- ¹⁸ LINEAR TECHNOLOGY, April 2015, [LTC1560-1](https://www.linear.com), URL www.linear.com
- ¹⁹ XMOS Ltd., startKIT development board, May 2015,
URL www.xmos.com/support/boards?product=17441&secure=1
- ²⁰ XMOS Ltd., April 2015, URL www.xmos.com
- ²¹ ANALOG DEVICES, April 2015, [AD9051](https://www.analog.com), URL www.analog.com

-
- ²² Steven W. Smith, The Scientist and Engineer's Guide to Digital Signal Processing, ISBN 0-9660176-3-3, ch2, p20
- ²³ XMOS Ltd., April 2015, [xTIMEcomposer](#) Community v13.2.2, URL www.xmos.com
- ²⁴ XMOS Ltd., GPIO Slice card, May 2015, URL www.xmos.com/support/boards?product=15831&secure=1
- ²⁵ Eltima Software, April 2015, [RS232 Data Logger](#), URL www.eltima.com
- ²⁶ Digilent Inc., April 2015, [Analog Discovery USB Oscilloscope](#), URL www.digilentinc.com
- ²⁷ Mathworks, MATLAB, Release R2014a, May 2015, URL www.mathworks.com
- ²⁸ Mathworks, MATLAB, Signal Processing Toolbox, May 2015, URL www.mathworks.com/products/signal/
- ²⁹ MathWorks, May 2015, URL [dsp.TimeScope System object](#), www.mathworks.com
- ³⁰ MathWorks, MATLAB medfilt1 function, May 2015, URL www.mathworks.com/help/signal/ref/medfilt1.html
- ³¹ MathWorks, MATLAB detrend function, May 2015, URL www.mathworks.com/help/matlab/ref/detrend.html
- ³² MathWorks, MATLAB pwelch function, May 2015, URL www.mathworks.com/help/signal/ref/pwelch.html?searchHighlight=pwelch
- ³³ MathWorks, MATLAB findpeaks function, May 2015, URL www.mathworks.com/help/signal/ref/findpeaks.html
- ³⁴ MathWorks, MATLAB spectrogram function, May 2015, URL www.mathworks.com/help/signal/ref/spectrogram.html
- ³⁵ Max Planck Institute for Gravitational Physics, Golm/Potsdam, Einstein Online, Chirping neutron stars, URL www.einstein-online.info/spotlights/chirping_neutron_stars
- ³⁶ B. Owen, Penn State University, Einstein Online, April 2015, URL www.einstein-online.info/spotlights/chirping_neutron_stars
- ³⁷ SETI@home, May 2015, URL setiathome.berkeley.edu